1-1-2014

Gain- or loss-induced localization in one-dimensional PT-symmetric tight-binding models

O. Vázquez-Candanedo

J. C. Hernández-Herrejón

F. M. Izrailev

D. N. Christodoulides
University of Central Florida

Gain- or loss-induced localization in one-dimensional $\mathcal{PT}$-symmetric tight-binding models

O. Vázquez-Candanedo,[1] J. C. Hernández-Herrejón,[2] F. M. Izrailev,[1,3] and D. N. Christodoulides[4]
[1]*Instituto de Física, Universidad Autónoma de Puebla, Apartado Postal J-48, Puebla, 72570 Mexico*
[2]*Instituto de Física, Universidad Autónoma de San Luis Potosí, Av. Manuel Nava 6, Zona Universitaria, 78290 Mexico*
[3]*NSCL and Department of Physics and Astronomy, Michigan State University, East Lansing, Michigan 48824-1321, USA*
[4]*CREOL/College of Optics, University of Central Florida, Orlando, Florida 32816, USA*
(Received 25 September 2013; published 24 January 2014)

We investigate the properties of parity-time ($\mathcal{PT}$)-symmetric tight-binding models by considering both bounded and unbounded models. For the bounded case, we obtain closed form expressions for the corresponding energy spectra and we analyze the structure of eigenstates as well as their dependence on the gain or loss contrast parameter. For unbounded $\mathcal{PT}$ lattices, we explore their scattering properties through the development of analytical models. Based on our approach we identify a mechanism that is responsible to the emergence of localized states that are entirely due to the presence of gain and loss. The derived expressions for the transmission and reflection coefficients allow one to better understand the role of $\mathcal{PT}$ symmetry in energy transport problems occurring in such $\mathcal{PT}$-symmetric tight-binding settings. Our analytical results are further exemplified via pertinent examples.

DOI: 10.1103/PhysRevA.89.013832 PACS number(s): 42.25.Bs, 42.82.Et, 11.30.Er

I. INTRODUCTION

Over the years the transport properties of Hermitian lattice systems have been a subject of intense investigation. Such arrangements are ubiquitous in nature and are typically characterized by succession of allowed bands and forbidden gaps [1]. They appear in many and diverse fields of physics and applied physics ranging from solid state, to Bose-Einstein condensates [2], to optical photonic crystals and lattices [3,4]. On the other hand, much less attention has been paid to nonconservative periodic structures. In this case, a configuration can in general exhibit either gain or loss and hence is non-Hermitian. While quantum mechanics is by nature Hermitian, gain or loss can be readily incorporated in classical settings. In the late 1990s, the notion of parity-time symmetry was first introduced by Bender and Boettcher within the framework of quantum field theory [5]. In this work it was shown that a broad family of Hamiltonians can exhibit entirely real spectra as long as they commute with the parity-time ($\mathcal{PT}$) operator and hence they may share a common set of eigenvectors. This is to some extent unexpected given that such properties are typically associated with Hermitian systems. In general, the eigenenergies of such arrangements are real only within a certain range of a non-Hermiticity parameter. Yet, once this parameter exceeds a critical threshold, the system can undergo a spontaneous symmetry breaking, corresponding to a transition from real to complex spectra thus entering the so-called broken $\mathcal{PT}$-symmetry regime [5,6]. Interestingly, this phase transition point exhibits all the characteristics of an exceptional point singularity.

In recent years the possibility of observing $\mathcal{PT}$-symmetric effects in optics has been suggested [7–10]. In this context $\mathcal{PT}$ symmetry can be readily established by requiring that the complex refractive index distribution obeys the relation $n(x) = n^{\star}(-x)$. In other words, this symmetry demands that the refractive index profile must be an even function of position while the gain or loss spatial distribution should be antisymmetric. As pointed out in several studies [11–29], $\mathcal{PT}$ symmetry can lead to a number of intriguing processes. These include for example band-merging effects in $\mathcal{PT}$-symmetric lattices [8], abrupt phase transitions [12], power oscillations and double refraction, and unidirectional invisibility [14,16,24]. In addition, nonreciprocal wave propagation is also possible when $\mathcal{PT}$ symmetry is used in conjunction with nonlinearity [19]. Other issues like defect states in $\mathcal{PT}$ lattices [14], the coexistence of coherent lasing-absorbing modes [17,23], and mode selection in $\mathcal{PT}$-symmetric lasers have also been investigated in the literature [25].

In this paper we present the results of a detailed study of the one-dimensional (1D) $\mathcal{PT}$-symmetric tight-binding model consisting of alternating gain or loss sites. One of our goals is to establish the relation between the properties of a bounded model with a finite number of sites, with those of scattering for the unbounded model, when the same structure is attached to perfect leads. Some aspects of this problem have already been discussed in the literature. In the short review [30] it was demonstrated how the methods that are well developed in nuclear and mesoscopic physics, can be used to describe the multiple scattering in non-Hermitian $\mathcal{PT}$-symmetric resonators with both absorbing and amplifying regions. The properties of scattering matrices in connection with the $\mathcal{PT}$-symmetry breaking points in the corresponding bounded systems have been recently analyzed in Ref. [31]. Other aspects of the bounded and unbounded $\mathcal{PT}$-symmetric models have been discussed in Refs. [18,20,32]. In our study we mainly focus on the structure of scattering states in relation to that of the eigenstates of a bounded model. We show that both the eigenstates of the bounded model and scattering states of the unbounded one can be analyzed in the unified approach; the difference is in the boundary conditions. Using our approach, we were able to derive the expression for the transmission coefficient that is valid for any values of the control parameters. This derivation is essentially based on the knowledge of the structure of scattering states, and not on the well-known method related to the evaluation of the product of transfer matrices [33].

Studying the structure of scattering states, we show that even without the presence of disorder one can speak about

the localization defined via the exponential decrease of the transmission coefficient. Although the physical effect of such a localization in the presence of a gain only (without absorption) is already studied, the mechanism of this unexpected effect was not fully understood. In our approach we show that in $\mathcal{PT}$-symmetric models a similar effect also emerges, however, it is much more complicated due to the interplay between gain and loss. By studying the structure of scattering states we have found that they are, indeed, exponentially localized under some conditions. In this case, the localization length of the scattering states (and not of the eigenstates of the isolated model that remain to be extended) is the same as that defined by the decrease of the transmission coefficient in the limit of a very large length of the scattering structure. Another goal of our study is to understand the role of the Bloch-like number, which in the presence of gain turns out to be quite specific. Since the approach we are using can be easily generalized to other physical models, we hope that our study will contribute to the general theory of $\mathcal{PT}$-symmetric systems.

II. THE MODEL

We consider the one-dimensional tight-binding model which is described by the standard Hamiltonian,

$$H_{mn} = \epsilon_n \delta_{mn} + v(\delta_{n,n+1} + \delta_{n,n-1}), \tag{1}$$

where v is the hopping amplitude connecting the nearest sites (in what follows we fix $v = 1$, a more general model with different left and right couplings was considered in Ref. [18]). As for imaginary on-site potential ϵ_n, its form is defined as follows,

$$\epsilon_n = \begin{cases} -i\gamma & \text{for } n \text{ odd}, \\ i\gamma & \text{for } n \text{ even}, \end{cases} \tag{2}$$

where $\gamma > 0$ stands for the loss (for n even) or for the gain (for n odd). This model can be treated as the bilayer model with alternating gain or loss sites, thus creating the structure belonging to the class of $\mathcal{PT}$-symmetric models revealing quite unexpected properties of scattering (see, for example [13,15,18,24,34,35],).

The Schrödinger equation with non-Hermitian Hamiltonian (1) takes the form,

$$i\hbar \frac{d\Psi_n(t)}{dt} = \Psi_{n+1}(t) + \Psi_{n-1}(t) + \epsilon_n \Psi_n(t). \tag{3}$$

The solution of this equation can be presented in the conventional form,

$$\Psi_n(t) = e^{-iEt}\psi_n, \tag{4}$$

with E as the energy of an eigenstate ψ_n. As will be shown, the energy E can be either real or complex (in fact, imaginary) depending on the value of γ. For non-Hermitian matrices there are two sets of eigenstates, left and right, however, we consider right eigenstates only. The relation between the two sets of eigenstates will be discussed below. Note also that there is a special case of $E = 0$ which we analyze separately.

Thus, we arrive at the stationary discrete Schrödinger equation,

$$E\psi_n = \psi_{n+1} + \psi_{n-1} + \epsilon_n \psi_n. \tag{5}$$

The general solution ψ_n of this equation can be written in the form,

$$\psi_n = \begin{cases} \delta(Ae^{ink} + Be^{-ink}) & \text{for } n \text{ odd}, \\ Ae^{ink} + Be^{-ink} & \text{for } n \text{ even}, \end{cases} \tag{6}$$

where the wave number k and constants A, B, δ to be expressed via the energy E and key parameter γ, either by the boundary conditions at $n = 0, 2N + 1$ for the *bounded model* or by the conditions at $n = -1, 0$ for the *unbounded model*. Here and below by bounded model we mean that apart from the gain or loss at the sites n, there is no coupling to continuum at the edges of a structure. In other words, this model corresponds to the problem of the dynamics of wave packets in the presence of fixed or periodic boundary conditions. Contrary, the unbounded model corresponds to the scattering problem for which the structure of size $2N$ is attached to perfect leads, and the main interest is in the transmission or reflection coefficient. By the direct substitution of Eq. (6) into Eq. (5) for both models the two parameters δ and k can be expressed in terms of energy E and control parameter γ as follows,

$$E + i\gamma = (2/\delta)\cos k, \quad E - i\gamma = 2\delta \cos k. \tag{7}$$

III. BOUNDED MODEL

A. Spectrum

Considering a system where for the sites $n = 1, \ldots, 2N$ the potential obeys Eq. (2) and taking zero boundary conditions at sites $n = 0$ and $n = 2N + 1$, i.e., $\psi_0 = \psi_{2N+1} = 0$, we have the relations,

$$A + B = 0, \quad Ae^{i(2N+1)k} + Be^{-i(2N+1)k} = 0, \tag{8}$$

which make the constants A and B linearly dependent and define discrete values for the parameter k,

$$k_s = \frac{s\pi}{2N+1}, \tag{9}$$

with $s = 1, \ldots, N$. Inserting k_s into Eq. (7) one can find the energy spectrum E_s which is defined by the relation,

$$4\cos^2 k_s = E_s^2 + \gamma^2. \tag{10}$$

To continue, it is useful to introduce the parameter β_s,

$$E_s = \pm 2 \cos k_s \sin \beta_s, \tag{11}$$

which can be expressed via k_s and γ,

$$\cos \beta_s = \frac{\gamma}{2\cos k_s}. \tag{12}$$

According to Eq. (7) δ can be written as

$$\delta_{\pm}^{(s)} = -ie^{\pm i\beta_s}. \tag{13}$$

The plus-minus signs in Eq. (11) stand to stress that for any value of k_s there are two values of energy symmetric with respect to the band center $E = 0$. From Eq. (12) one can see that β_s can take real or imaginary values depending on whether

γ is smaller or larger than $2\cos k_s$, respectively. Therefore, the energy E_s in Eq. (11) can be either real or purely imaginary, the result which is entirely due to the $\mathcal{PT}$ symmetry of our gain or loss potential.

Let us now analyze the properties of the energy spectrum in dependence on the parameter γ for a fixed N. From Eq. (12) one gets that all eigenvalues are real for $\gamma < 2\cos k_s$ for any value of s. Since the smallest value of $\cos k_s$ occurs for $s = N$, the condition of a completely real spectrum is

$$\gamma < \gamma_{\rm cr}^{(1)} = 2\cos\left(\frac{N\pi}{2N+1}\right) \approx \frac{\pi}{2N}, \qquad (14)$$

where the estimate for $N \gg 1$ is also given. A typical example of such spectrum is shown in Fig. 1(a) for $\gamma = 0.05$ and $N = 10$, for which $\gamma_{\rm cr}^{(1)} = 0.157$. Note that in this case imaginary parts of E_s vanish.

On the other hand, when

$$\gamma > \gamma_{\rm cr}^{(2)} = 2\cos\left(\frac{\pi}{2N+1}\right) \approx 2\left(1 - \frac{\pi^2}{8N^2}\right), \qquad (15)$$

all values of E_s are imaginary. Therefore, for $\gamma_{\rm cr}^{(1)} < \gamma < \gamma_{\rm cr}^{(2)}$ some of the eigenvalues E_s are real and others are imaginary; see Fig. 1(a). The data in this figure demonstrate that all eigenvalues E_s are combined in pairs, having the symmetry (with respect to zero) either for real or pure imaginary values. From Fig. 1 one can understand the dynamics of energy levels upon the increase of γ. For $\gamma = 0$ all values of E_s are real in the range $-2 < E_s < 2$ and correspond to those emerging in the perfect lattice. With an increase of γ, two eigenvalues mostly close to the band center start to move to zero, and after they continue to move along the imaginary axes, one moves up and another moves down. The critical point $\gamma = \gamma_{\rm cr}^{(1)}$ is known in literature as an *exceptional point*.

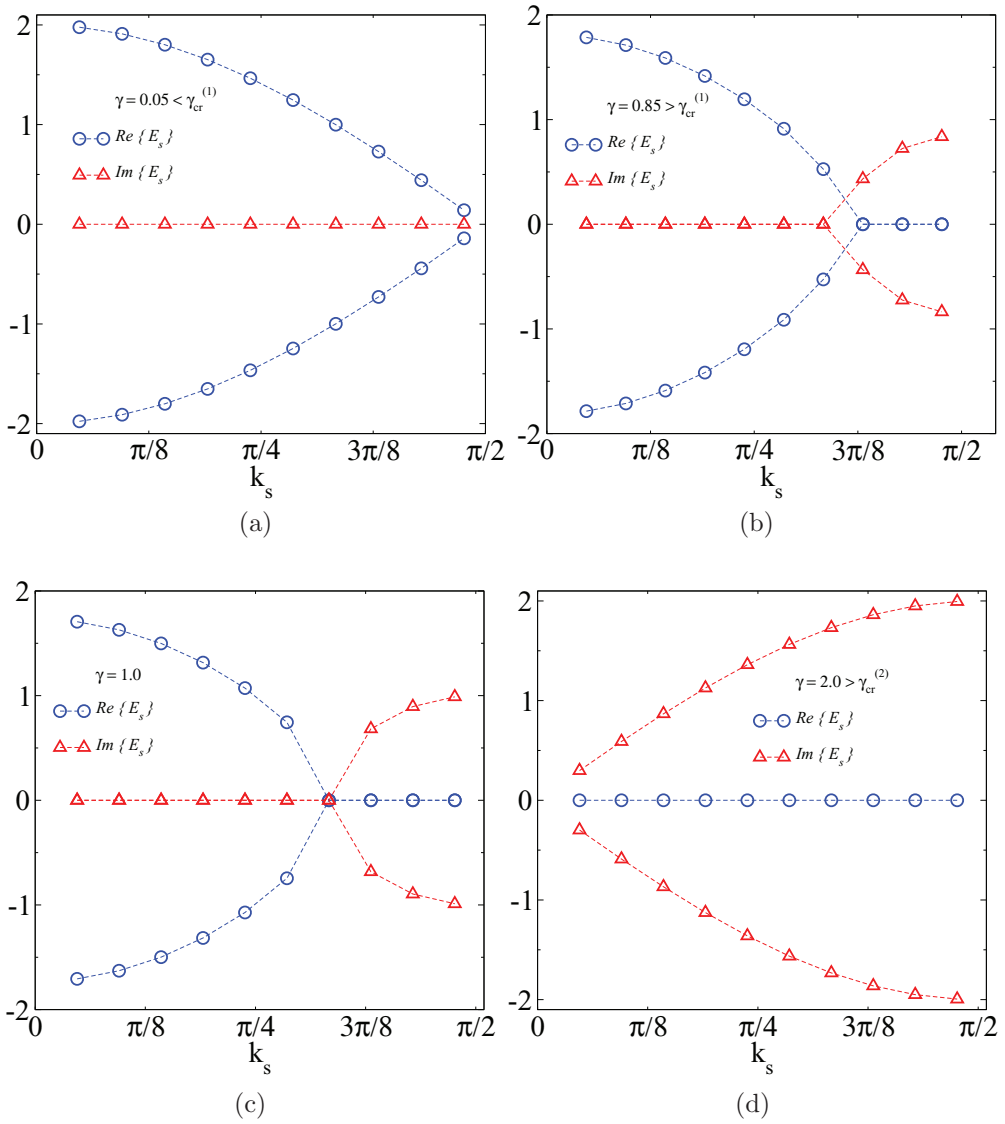

FIG. 1. (Color online) Energy spectrum E_s as a function of k_s for $N = 10$. (a) $\gamma = 0.05$ with $\gamma < \gamma_{\rm cr}^{(1)}$, therefore, all eigenvalues are real; (b) $\gamma = 0.85$ with $\gamma > \gamma_{\rm cr}^{(1)}$ for which there are both real and imaginary eigenvalues; (c) $\gamma = \gamma_{\rm cr} = 1.0$ for $s = N - 3$, such that two eigenvalues coalesce at the band center; (d) $\gamma = 2.0$ with $\gamma > \gamma_{\rm cr}^{(2)}$ when all eigenvalues are imaginary.

With further increase of γ the second pair of real eigenvalues closest to $E = 0$ approaches the band center. When passing the corresponding critical value (second exceptional point) for this pair of E_s, one eigenvalue goes up along the imaginary axes, and another goes down. This scenario continues with an increase of γ, and when $\gamma > \gamma_{\rm cr}^{(2)}$ all the values E_s are purely imaginary. It is clear that in the limit $N \to \infty$, the critical value $\gamma_{\rm cr}^{(1)}$ vanishes, thus indicating that the phase in which all eigenvalues are real, is absent; see Figs. 2(a) and 2(b).

B. Eigenstates

For non-Hermitian Hamiltonians with a discrete spectrum there are two sets of eigenstates, left ($\psi_l^{(s)}$) and right ($\psi_r^{(s)}$) defined by the equations,

$$H\psi_r^{(s)} = E_s\psi_r^{(s)}, \quad \psi_l^{(s)}H = E^s\psi_l^{(s)}, \tag{16}$$

with, in general, complex conjugate eigenvalues, $E^s = E_s^*$ [36]. Since $\psi_l^{(s)} = (\psi_r^{(s)})^*$ we explore one set of eigenstates only. In what follows we solve the first of Eq. (16) only, determining the structure of right eigenstates. For this reason we omit the index r for right eigenstates.

To start with the global structure of eigenstates in connection with the properties of spectra, first, one has to understand the symmetric properties of eigenstates. Because the parameter δ in Eq. (13) takes two values, there are two types of eigenstates, ψ_n^+ and ψ_n^-. The right eigenstates can be obtained by applying the conditions obtained from Eq. (8) to Eq. (6), which gives

$$\psi_n^{(s)\pm} = \begin{cases} 2i\delta_\pm^{(s)}A_\pm^{(s)}\sin(nk_s) & \text{for } n \text{ odd}, \\ 2iA_\pm^{(s)}\sin(nk_s) & \text{for } n \text{ even}. \end{cases} \tag{17}$$

Here $A_\pm^{(s)}$ is a constant that can be determined by the normalization condition.

1. Eigenstates for $\gamma < 2\cos k_s$

For $\gamma < 2\cos k_s$ the parameter β_s is real; see Eq. (12). Normalizing the eigenstates such that $\sum_{n=1}^{2N}|\psi_n^{(s)\pm}|^2 = 1$ one gets

$$|A_+^{(s)}|^2 = |A_-^{(s)}|^2 = \frac{1}{\zeta^2}, \tag{18}$$

where

$$\zeta = \sqrt{2(2N+1)}. \tag{19}$$

Note that the factors $A_\pm^{(s)}$ are determined up to some phase which we chose in such a way that for $\gamma = 0$ the standard expressions for eigenstates in the perfect lattice are recovered. Therefore, by introducing the following relations,

$$A_+^{(s)} = \frac{e^{-i\beta_s}}{\zeta}, \quad \nu_s = \frac{\pi}{2} - \beta_s, \quad \mathcal{D} = \frac{2}{\zeta}, \tag{20}$$

the states $\psi_n^{(s)+}$ for positive $E_s > 0$ get the form,

$$\psi_n^{(s)+} = \begin{cases} \mathcal{D}\sin(nk_s) & \text{for } n \text{ odd}, \\ e^{i\nu_s}\mathcal{D}\sin(nk_s) & \text{for } n \text{ even}. \end{cases} \tag{21}$$

In the same way, by introducing

$$A_-^{(s)} = \frac{i}{\zeta}, \tag{22}$$

the other set $\psi_n^{(s)-}$ of eigenstates with negative energies, $E_s < 0$, is defined by

$$\psi_n^{(s)-} = \begin{cases} e^{i\nu_s}\mathcal{D}\sin(nk_s) & \text{for } n \text{ odd}, \\ -\mathcal{D}\sin(nk_s) & \text{for } n \text{ even}. \end{cases} \tag{23}$$

An example of eigenstates for energies $E_s = \pm 1.46$ is shown in Fig. 3 for a system with $\gamma = 0.05$ and $N = 10$. The most important issue of such eigenstates with real energies is that all of them are extended in the site representation. This fact is due to the fixed boundary conditions, as it also happens in classical chains of linear oscillators (similar

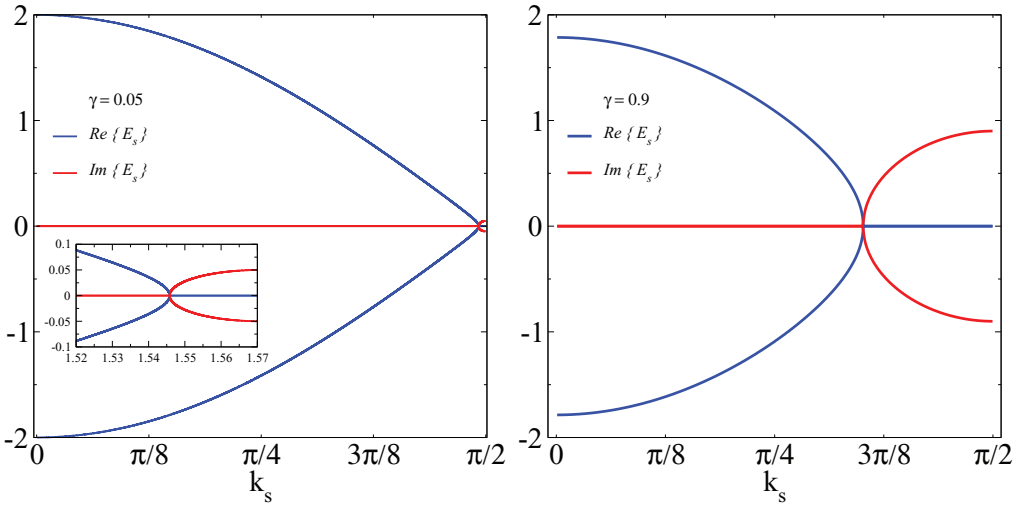

(a) (b)

FIG. 2. (Color online) Energy spectrum for system with $N \to \infty$. (a) Spectrum for $\gamma = 0.05$ (inset shows zoom of the region around critical value); (b) spectrum for $\gamma = 0.9$.

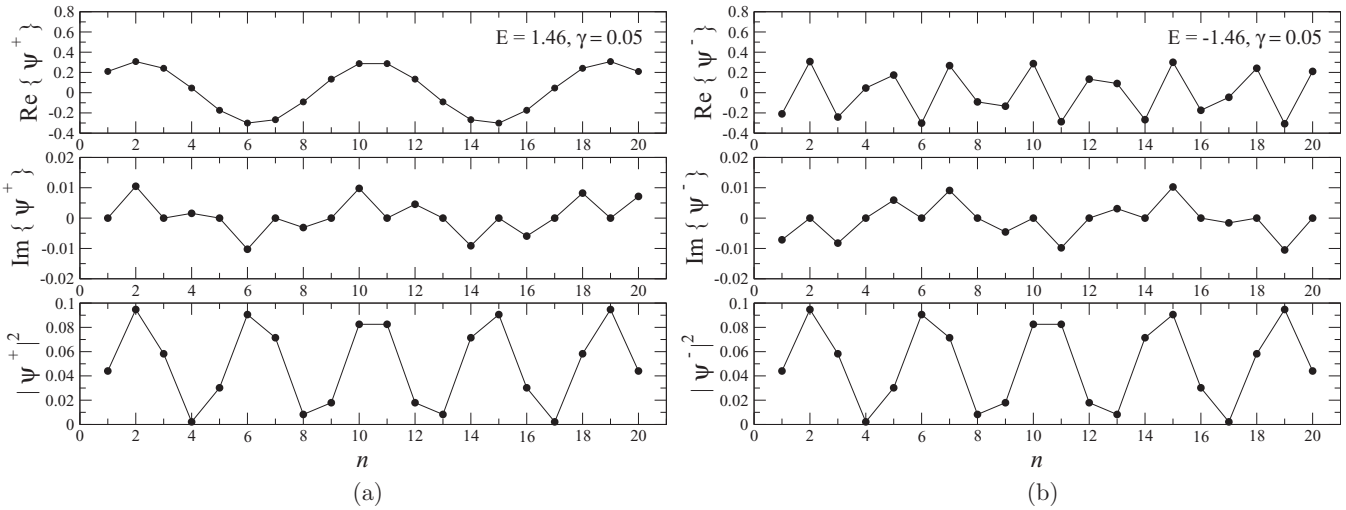

FIG. 3. The eigenstates corresponding to the energy $E_s = 1.46$ (left panel), and to $E_s = -1.46$ (right panel) for a system with $\gamma = 0.05$ and $N = 10$.

structure occurs for periodic boundary conditions). As for the time-dependent part of the solution $\Psi_n(t)$ [see Eq. (4)], since the energies E_s are real, each site oscillates with the same frequency.

The detailed analysis of the eigenstates shows quite interesting symmetries between $\psi_n^{(s)+}$ and $\psi_n^{(s)-}$. Specifically, for n odd one can reveal the relations,

$$\psi_n^{(s)+} = \begin{cases} \left(\psi_{2N-n+1}^{(s)-}\right)^*, & \text{for } s \text{ odd}, \\ -\left(\psi_{2N-n+1}^{(s)-}\right)^*, & \text{for } s \text{ even}. \end{cases} \tag{24}$$

Correspondingly, for n even one gets

$$\psi_n^{(s)+} = \begin{cases} -\mathrm{Re}\left\{\left(\psi_{2N-n+1}^{(s)-}\right)^*\right\} + \mathrm{Im}\left\{\left(\psi_{2N-n+1}^{(s)-}\right)^*\right\}, & \text{for } s \text{ odd}, \\ \mathrm{Re}\left\{\left(\psi_{2N-n+1}^{(s)-}\right)^*\right\} - \mathrm{Im}\left\{\left(\psi_{2N-n+1}^{(s)-}\right)^*\right\}, & \text{for } s \text{ even}. \end{cases} \tag{25}$$

These symmetries can be seen in Fig. 3 under a close inspection.

2. *Eigenstates for* $\gamma > 2\cos k_s$

According to Eq. (12) in this case β_s is imaginary, therefore, $\beta_s = i\tilde{\beta}_s$ with $\tilde{\beta}_s$ real. The normalization will be now given by

$$|A_\pm^{(s)}|^2 = \frac{1}{\zeta_\pm^{(s)2}}, \tag{26}$$

where

$$\zeta_\pm^{(s)} = \sqrt{(e^{\mp 2\tilde{\beta}_s} + 1)(2N+1)}. \tag{27}$$

By introducing

$$A_+^{(s)} = \frac{-i}{\zeta_+^{(s)}} \quad \text{and} \quad \mathcal{D}_+ = \frac{2}{\zeta_+^{(s)}}, \tag{28}$$

the eigenstate $\psi_n^{(s)+}$ for positive imaginary part $\mathrm{Im}\{E_s\} > 0$ can be presented in the form,

$$\psi_n^{(s)+} = \begin{cases} i\mathcal{D}_+ e^{-\beta_s} \sin(nk_s) & \text{for } n \text{ odd}, \\ \mathcal{D}_+ \sin(nk_s) & \text{for } n \text{ even}. \end{cases} \tag{29}$$

Also, by using

$$A_-^{(s)} = -\frac{1}{\zeta_-^{(s)}} \quad \text{and} \quad \mathcal{D}_- = \frac{2}{\zeta_-^{(s)}}, \tag{30}$$

the other set $\psi_n^{(s)-}$ of eigenstates with negative imaginary part, $\mathrm{Im}\{E_s\} < 0$, takes the form,

$$\psi_n^{(s)-} = \begin{cases} \mathcal{D}_- e^{\beta_s} \sin(nk_s) & \text{for } n \text{ odd}, \\ -i\mathcal{D}_- \sin(nk_s) & \text{for } n \text{ even}. \end{cases} \tag{31}$$

Figure 4 demonstrates the structure of two eigenstates corresponding to energy $E_s = \pm i 0.133$, for a system with $\gamma > 2\cos k_N$ and $N = 10$. In this case there are only two eigenstates with imaginary energies. One can see that according to Eqs. (29) and (31) both eigenstates are extended in the position representation. However, in contrast with the previous case of real energies E_s now the modes $\Psi_n(t)$ are either exponentially increasing or decreasing in time, depending on the sign of the imaginary part of the eigenvalues.

In Fig. 4 the symmetry between $\psi_m^{(s)+}$ and $\psi_m^{(s)-}$ is quite simple; this is due to the fact that for the chosen parameters, $\tilde{\beta}_s \approx 0$ and $\mathcal{D}_+ \approx \mathcal{D}_-$. However, as γ grows this symmetry disappears.

3. *Eigenstates for* $\gamma = 2\cos k_s$

For the case when $\gamma = 2\cos k_s$ two eigenvalues approach the band center, $E = 0$, from the left and right and the value of β_s vanishes. At this exceptional point the corresponding eigenstates are related to each other due to the simple relation, $\psi_n^{(s)+} = i\psi_n^{(s)-}$; see Eqs. (21) and (23). The example of such eigenstates is given in Fig. 5 for a system with $\gamma = \gamma_{\mathrm{cr}}^{(1)}$

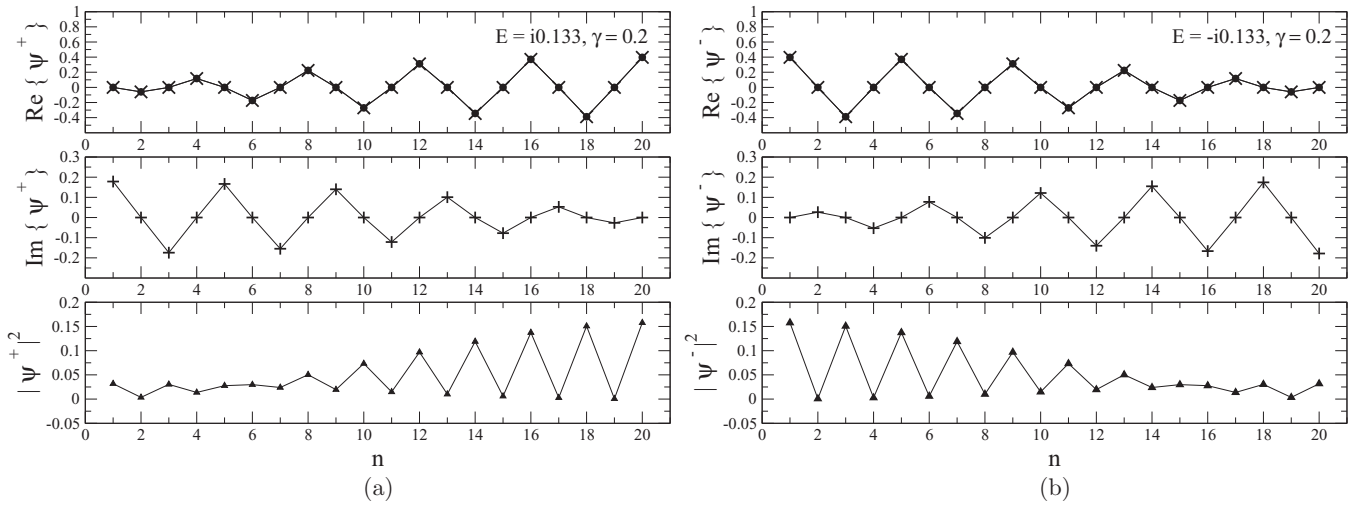

FIG. 4. Eigenstates corresponding to energies $E_s = \pm i0.133$, for a system with $\gamma > 2\cos k_N$, $N = 10$ and $\gamma = 0.2$.

and $N = 10$. As one can see, for this specific case the corresponding solution of the time-dependent equation (3) does not depend on time, $\Psi_n(t) \sim \psi_n^{(s)\pm}$. However, this is not the only solution of Eq. (3), there is an additional solution which linearly depends on time, $\Psi_n(t) \sim t\psi_n^{(s)\pm}$. This fact can be easily confirmed by the direct evaluation of Eq. (3). The consequence of this result for the wave-packet dynamics has been discussed in Ref. [24].

IV. UNBOUNDED MODEL

A. Scattering states

Below we consider the problem of transmission through the bounded model with the $\mathcal{PT}$-symmetric potential defined by Eq. (2) for $n = 1, \ldots, 2N$, with N standing for the total number of basic cells. In contrast with the bounded model, now we assume that the model is attached to perfect semi-infinite leads, specifically, $\epsilon_n = 0$ for $n > 2N$ and $n \leqslant 0$. We also assume an incoming plane wave from the right side of the system, therefore, the left lead is occupied by the transmitted wave only. One can use the transfer matrix approach which allows one to find ψ_{2N+1} and ψ_{2N} due to the following relation,

$$\begin{pmatrix} \psi_{2N+1} \\ \psi_{2N} \end{pmatrix} = \mathcal{M}^N \begin{pmatrix} \psi_1 \\ \psi_0 \end{pmatrix}, \qquad \mathcal{M} = \begin{pmatrix} E - i\gamma & -1 \\ 1 & 0 \end{pmatrix} \begin{pmatrix} E + i\gamma & -1 \\ 1 & 0 \end{pmatrix}. \tag{32}$$

As one can see, the problem is reduced to the corresponding dynamical system,

$$\begin{pmatrix} \psi_{n+1} \\ \psi_n \end{pmatrix} = \begin{pmatrix} E - i\gamma & -1 \\ 1 & 0 \end{pmatrix} \begin{pmatrix} E + i\gamma & -1 \\ 1 & 0 \end{pmatrix} \begin{pmatrix} \psi_{n-1} \\ \psi_{n-2} \end{pmatrix} = \mathcal{M} \begin{pmatrix} \psi_{n-1} \\ \psi_{n-2} \end{pmatrix}, \tag{33}$$

for "n" *even*. Note that in this representation the index n denoting the sites can be treated as the discrete "time." The solution can be written in terms of eigenvectors $\vec{\xi}_1, \vec{\xi}_2$ and

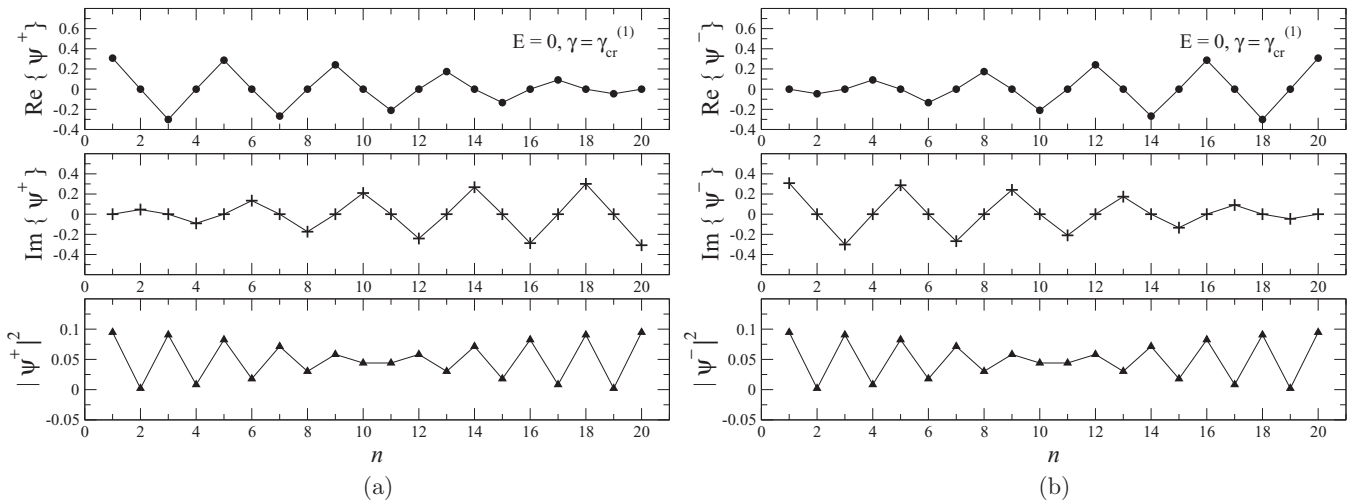

FIG. 5. Degenerate eigenstates corresponding to energy $E_s = 0$, for a system with $\gamma = \gamma_{\rm cr}^{(1)}$ and $N = 10$.

eigenvalues λ_1,λ_2 of the matrix $\mathcal{M}$,

$$\begin{pmatrix}\psi_{n+1}\\ \psi_n\end{pmatrix} = B\lambda_1^{n/2}\overrightarrow{\xi_1} + A\lambda_2^{n/2}\overrightarrow{\xi_2}, \tag{34}$$

with constants A and B determined by the initial conditions [33],

$$\psi_0 = 1, \quad \psi_1 = e^{-ik}. \tag{35}$$

One can show that the eigenvalues of matrix $\mathcal{M}$ are given by

$$\lambda_{1,2} = \frac{E^2+\gamma^2}{2} - 1 \mp \frac{1}{2}\sqrt{(E^2+\gamma^2-2)^2-4}, \tag{36}$$

and the corresponding eigenvectors are

$$\overrightarrow{\xi_1} = \begin{pmatrix}\frac{1+\lambda_1}{E+i\gamma}\\ 1\end{pmatrix}, \quad \overrightarrow{\xi_2} = \begin{pmatrix}\frac{1+\lambda_2}{E+i\gamma}\\ 1\end{pmatrix}. \tag{37}$$

Using the parametrization, similar to that in Eqs. (11)–(13),

$$E = 2\cos\mu\sin\beta, \quad \frac{\gamma}{2\cos\mu} = \cos\beta, \quad \delta = -ie^{i\beta}, \tag{38}$$

the eigenvalues and eigenvectors can be written as follows,

$$\lambda_{1,2} = e^{\mp 2i\mu}, \tag{39}$$

and

$$\overrightarrow{\xi_1} = \begin{pmatrix}\delta e^{-i\mu}\\ 1\end{pmatrix}, \qquad \overrightarrow{\xi_2} = \begin{pmatrix}\delta e^{i\mu}\\ 1\end{pmatrix}. \tag{40}$$

Here it is important to stress the difference between the problem of spectrum and eigenstates (for bounded model), and the scattering problem (for the unbounded model). In the former we fix the parameter γ and boundary conditions, in order to obtain the corresponding energy levels. In contrast, the (real) energy E in the scattering problem is the energy of the scattering wave, therefore, it is a free parameter. The physical meaning of μ can be compared with that of the Bloch wave number that emerges in 1D periodic structures with $N \to \infty$. In our model N can get any value, nevertheless, the variable μ plays the role of a wave number inside the sample. According to the dispersion relation,

$$4\cos^2\mu = E^2+\gamma^2, \tag{41}$$

the value of μ can be either real or imaginary depending on whether $E^2+\gamma^2 \leqslant 4$ or $E^2+\gamma^2 > 4$, respectively. We have to note that in contrast with the bounded model the parameter δ has one sign only due to specific conditions (35) for ψ_0 and ψ_1 corresponding to the *iteration*of ψ_n from the left to right side of the sample. Note, however, that the *propagation* of the scattering wave occurs from the right to left side of the structure.

By inserting Eqs. (40) and (39) into Eq. (34) we get

$$\begin{aligned}\psi_{n+1} &= \delta(Ae^{i(n+1)\mu} + Be^{-i(n+1)\mu}),\\ \psi_n &= Ae^{in\mu} + Be^{-in\mu},\end{aligned} \tag{42}$$

with "n" *even*. These expressions are of the same form as Eq. (6), however, they have different meaning. In contrast with Eq. (6) defining the eigenstates of the stationary Schrödinger equation, here ψ_n are components of scattering states inside the sample attached to the leads.

In order to determine the constants A and B one has to use the initial conditions (35). As a result, we obtain

$$A = \frac{ie^{-i\beta}e^{-ik} - e^{-i\mu}}{2i\sin\mu}, \quad B = 1 - \frac{ie^{-i\beta}e^{-ik} - e^{-i\mu}}{2i\sin\mu}. \tag{43}$$

Equations (42) and (43) fully determine the scattering states for $\mu \neq 0$, for both real and imaginary value of μ. Figure 6 shows the structure of the scattering states in both cases. In the former case the on-site probabilities inside the sample are periodic functions with respect to the index n. In contrast, when μ is imaginary, there are two terms in the expression for on-site probabilities, one of which is an exponentially increasing function of n, and another is a decreasing function. Therefore, formally one can speak about the localization of scattering states, and the exponential decrease of T for $E^2+\gamma^2 > 4$ can be directly related to the localization length. Note that such a

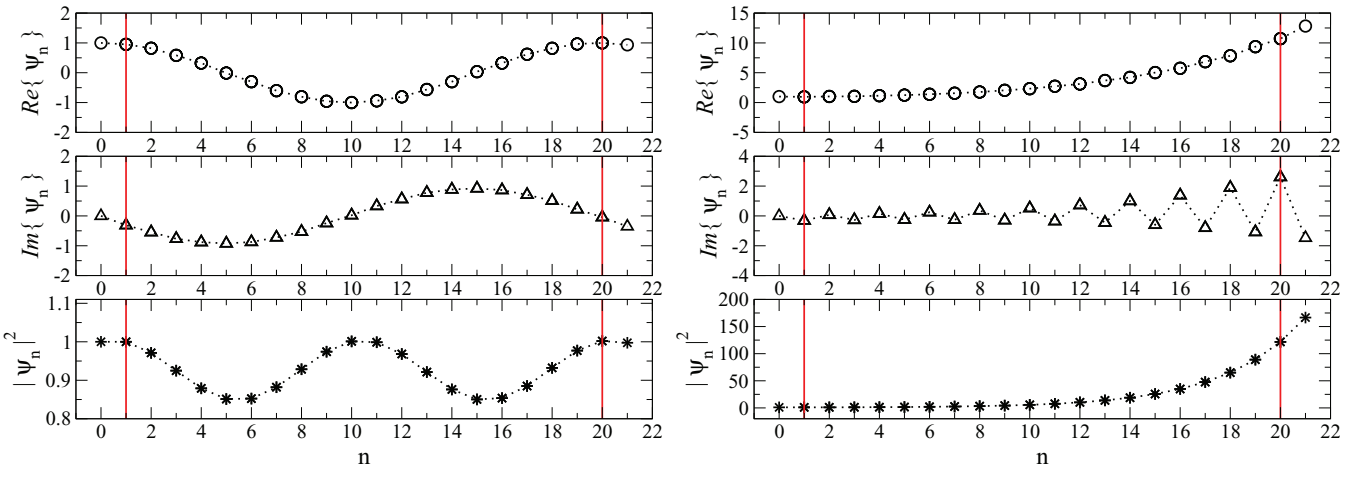

FIG. 6. (Color online) Scattering states for $E = 1.9$ and $N = 10$. (a) Scattering state for $\gamma = 0.05$ such that $E^2+\gamma^2 < 4$ and μ real. (b) Scattering state for $\gamma = 0.7$ such that $E^2+\gamma^2 > 4$ and μ imaginary.

localization occurs in the absence of disorder, the fact which has been noticed when discussing the properties of scattering for the model with constant gain or loss only [32,37–45].

We can get an estimate of the rate of increase of $|\psi_n|^2$ with the use of Eqs. (42) and (43) applied to the case when $E^2+\gamma^2>4$. By introducing $\mu=i\phi$ for $\phi>0$, it is sufficient to analyze only the scattering state for even sites,

$$|\psi_n|^2 = e^{2n\phi}\left(\frac{C_1}{2}+C_2+1\right)+e^{-2n\phi}\left(\frac{C_1}{2}\right)-C_1-C_2, \tag{44}$$

where

$$C_1=\frac{[\cosh\phi-\sin(\beta+k)]e^{\phi}}{\sinh^2\phi}, \quad C_2=\frac{\sin(\beta+k)-e^{\phi}}{\sinh\phi}. \tag{45}$$

Taking $n\gg 1$, one gets

$$|\psi_n|^2 \propto e^{2n\phi}, \tag{46}$$

therefore, the rate of exponential increase is given by 2ϕ. Correspondingly, the localization length can be defined as

$$\frac{1}{\ell_\infty}=2\phi\approx\sqrt{E^2+\gamma^2-4}. \tag{47}$$

Here the estimate is given for $\gamma\ll 1$. Since in this case the energy E has to be close to the band edge $E=\pm 2$, one can write $|E|=2-\Delta$ where Δ is the distance from the band edge. By assuming $\gamma^2\gg 4\Delta$, one can get the simplified estimate for the localization length, $\ell_\infty\approx 1/\gamma$.

For the special case with $E^2+\gamma^2=4$ we have $\mu=0$, and from Eq. (42) one gets $A=1$ and $B=0$. Therefore, the on-site probabilities $|\psi_n|^2$ are all equal to unity as Fig. 7 clearly manifests. As is expected, and will be shown rigorously below, the transmission coefficient T in this case equals 1. Since $\mu=0$, this means that in this case the wave propagates through the structure of size N without change of its phase. Thus, such a structure will be nonvisible for an observer.

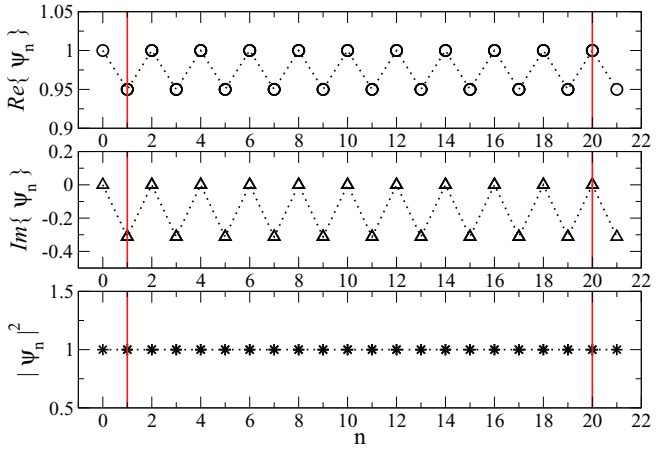

FIG. 7. (Color online) Scattering state for $E=1.9$, $N=10$, and $\gamma=0.6245$ such that $E^2+\gamma^2=4$ and $\mu=0$.

B. Transmittance

According to the general theory [33], the transmission coefficient T can be expressed as follows,

$$T=\frac{1}{|(\mathbf{M}^{(N)})_{22}|^2}. \tag{48}$$

Here the matrix $\mathbf{M}^{(N)}$ emerges when the relation (32) is written in the representation of plane waves,

$$Q^{-1}\begin{pmatrix}\psi_{2N+1}\\ \psi_{2N}\end{pmatrix}=Q^{-1}\mathcal{M}^{(N)}QQ^{-1}\begin{pmatrix}\psi_1\\ \psi_0\end{pmatrix} =\mathbf{M}^{(N)}Q^{-1}\begin{pmatrix}\psi_1\\ \psi_0\end{pmatrix}, \tag{49}$$

where

$$Q=\begin{pmatrix}1 & 1\\ e^{-ik} & e^{ik}\end{pmatrix}. \tag{50}$$

After standard manipulations one can express the transmission coefficient T in terms of ψ_{2N} and ψ_{2N+1} (see details in Ref. [33]),

$$T=\frac{4\sin^2 k}{|e^{-ik}\psi_{2N+1}-\psi_{2N}|^2}. \tag{51}$$

In this expression k is the wave number of incoming wave, and the values of ψ_1 and ψ_0 have to be specified due to Eq. (35). As is discussed above, the meaning of these initial values is due to fixing the plane wave propagating to the *left* from the sample (for $n\leqslant 1$), after an incoming wave (electron) comes from the *right* of the sample (for $n>2N$). Note that here the index N corresponds to the cell consisting of two sites with alternating gain and loss. Therefore, the total number of cells in the scattering structure is $2N$.

Note that in contrast with the bounded model, here $E=2\cos k$ is the energy of incoming plane wave, expressed through the wave vector k. In order to obtain an expression for T as a function of the parameters γ, E, and N, we insert the expressions defined by Eq. (42) into Eq. (51), with the constants A and B given by Eq. (43). After some technical work, one can represent the transmission coefficient in a quite compact form,

$$T=\frac{1}{1-\frac{\gamma^2}{4\sin^2 k\cos^2\mu}\sin^2(2\mu N)}. \tag{52}$$

This result is exact and valid for any values of control parameters, E and γ for a fixed N. Let us discuss the main properties of the transmission with the use of this expression. First, one has to recall the relation for the Bloch-like index μ,

$$4\cos^2\mu=E^2+\gamma^2, \qquad \mu=\begin{cases}\text{real} & \text{for} \quad E^2+\gamma^2<4,\\ \text{zero} & \text{for} \quad E^2+\gamma^2=4,\\ \text{imaginary} & \text{for} \quad E^2+\gamma^2>4,\end{cases} \tag{53}$$

with $2\cos k=E$. One can see that when μ is real the transmission T is a *periodic* function of N. To the contrary, when μ is imaginary, $\mu=i\phi$ $(\phi>0)$, we have $\cos\mu=\cosh\phi$, and $\sin(2\mu N)=i\sinh(2\phi N)$. Therefore, $\ln T$ takes

negative values resulting in its *monotonic decrease* with an increase of N. From the theory of disordered systems the exponential decrease of T with the system size N is a specific property of the Anderson localization. Here, we also can define the localization length with the use of the standard relation,

$$\frac{1}{\ell_\infty} = -\lim_{N\to\infty}\frac{\ln T}{2N}, \tag{54}$$

and treat the quantity ℓ_∞ as the localization length. When μ takes imaginary values, $\mu = i\phi$, the logarithm of the transmission coefficient can be written in the form,

$$\begin{aligned} \ln T &= -\ln(1-2D+D(e^{4\phi N}+e^{-4\phi N})), \\ D &= \frac{\gamma^2}{16\sin^2 k\cosh^2\phi}. \end{aligned} \tag{55}$$

First, from these relations one can easily see that $\ln T$ is always negative, therefore, the transmission coefficient T is less than one. Second, for imaginary μ a pure exponential decrease of T occurs for sufficiently large values of $N \geqslant N_{\rm cr}$, and not for any N as it happens in the disordered models without gain. The estimate of $N_{\rm cr}$ can be easily obtained from the above expression, it gives $N_{\rm cr} \approx 1/\phi$. For $N \geqslant N_{\rm cr}$ one gets

$$\ln T \approx -\ln D - 4\phi N. \tag{56}$$

Therefore, in the limit $N \to \infty$ we arrive at the expression (47) for the localization length ℓ_∞ characterizing an exponential decrease of the scattering wave propagating from the right to left of the structure.

As one can see from Eq. (52), the transmission coefficient T equals unity for $\mu = 0$ which leads to the relation $E^2 + \gamma^2 = 4$ between the energy E and the parameter γ. For a fixed energy E this relation defines the critical value $\gamma_{\rm cr}$,

$$E^2 + \gamma_{\rm cr}^2 = 4, \tag{57}$$

such that for $\gamma < \gamma_{\rm cr}$ the parameter μ is real, therefore, the dependence of $\ln T$ is a periodic function of N; see Fig. 8. Note that in this case the transmission coefficient is larger than 1, apart from the set of resonances with $T = 1$, defined by the relation $N \approx m\pi/2\mu$ with m as positive integer. The maximum value of T observed in this regime is located at the points $N \approx m\pi/4\mu$ with m positive odd integers, leading to the value $\ln T = -\ln(1 - \frac{\gamma^2}{4\sin^2 k\cos^2\mu})$. For $\gamma > \gamma_{\rm cr}$ the value of μ is imaginary, therefore, the transmission T decreasing with an increase of N; see Fig. 8. Note that for specific value $\gamma = \gamma_{\rm cr}$ the logarithm of the transmission coefficient vanishes for *any* N. The right panel of Fig. 8 demonstrates that for $N \leqslant N_{\rm cr} \approx 20$ *both* increasing and decreasing components of the scattering state essentially contribute to the value of T.

The behavior of $\ln T$ as a function of E can be seen in Fig. 9 for the case $N = 2$ (therefore, with four sites). Here we can see that as E approaches the band edges the transmission coefficient vanishes. One can detect the resonant energies E_r for which $T = 1$. In general, they are given by the expression,

$$E_r = \pm\sqrt{4\cos^2\left(\frac{m\pi}{2N}\right) - \gamma^2}, \quad (m = 0,1,\ldots,N). \tag{58}$$

Note that the number of such resonances in dependence on the energy depends not only on N but also on the parameter γ, because E_r is real only when $4\cos^2(\frac{m\pi}{2N}) > \gamma^2$. Therefore, for a sufficiently large γ all resonances may disappear. Also we would like to note that the first resonance emerging for $m = 0$ corresponds to $\mu = 0$, at this point $\ln T$ changes its sign.

Finally, by Fig. 10 we demonstrate the behavior of $\ln T$ as a function of γ. Here again one can see the resonances defined by the relation,

$$\gamma_r = \sqrt{4\cos^2\left(\frac{m\pi}{2N}\right) - E^2}, \quad (m = 0,1,\ldots,N). \tag{59}$$

The total number of these resonances is determined by the size N of the sample and by the energy E. One can see that for

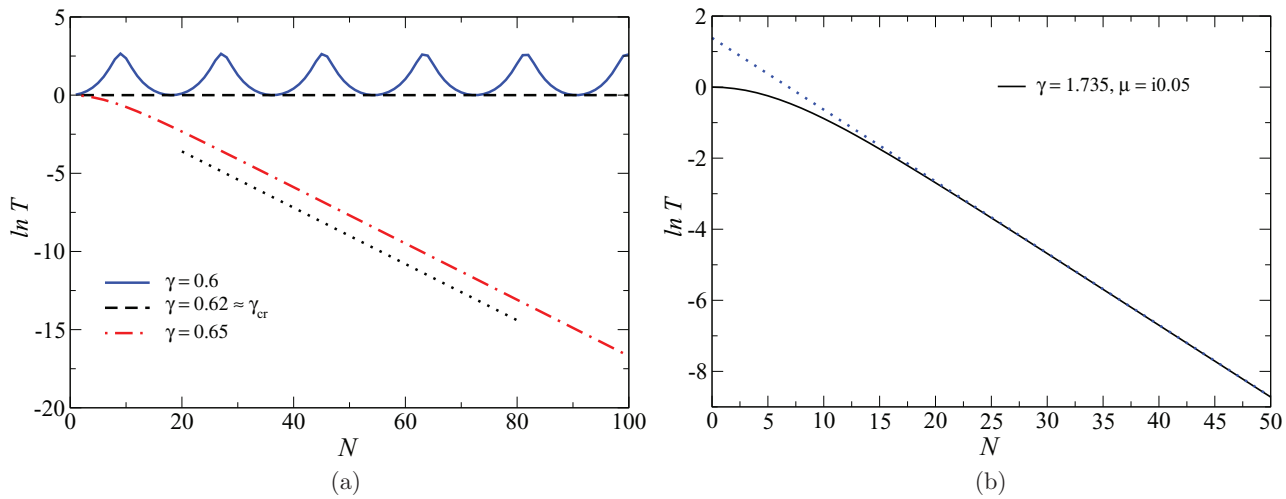

FIG. 8. (Color online) (Left panel) The N dependence of $\ln T$ for $\gamma = 0.6, 0.62, 0.65$, and fixed energy $E = 1.9$. When $\gamma < \gamma_{\rm cr} \approx 0.62$, the logarithm of T is a positive periodic function with the fundamental period $\pi/2\mu$. When $\gamma \approx \gamma_{\rm cr}$ we have $\ln T = 0$. Finally, when $\gamma > \gamma_{\rm cr}$, the value of $\ln T$ is negative, with a monotonically decreasing dependence. (Right panel) The N dependence of $\ln T$ for $\gamma = 1.735$ and $E = 1.0$. In this case μ is imaginary, and for $N \leqslant N_{\rm cr}$ both increasing and decreasing components of the scattering state make strong contribution to T. On both panels the dotted line shows the analytic estimate of $\ln T$ for $\gamma > \gamma_{\rm cr}$.

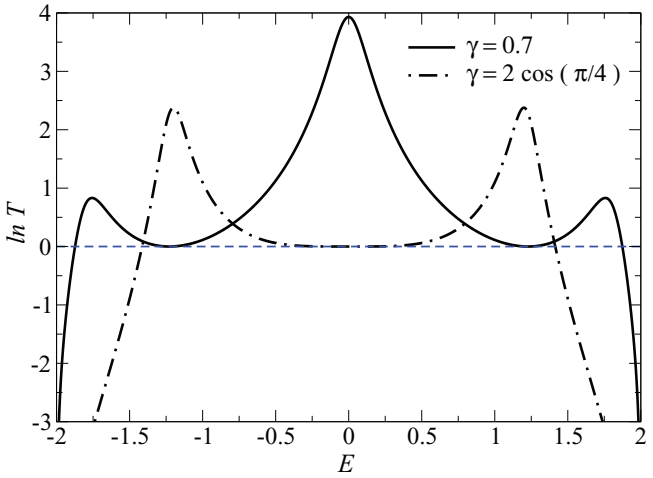

FIG. 9. (Color online) Energy dependence of $\ln T$ for $N = 2$ with $\gamma = 0.7$ and $\gamma = 2\cos(\pi/4)$. Note that for the latter value of γ, $T \approx 1$ in a quite large region of energy around $E = 0$.

$N = 2$, the transmission for small γ is close to unity practically for any energy.

C. Reflectance

The analytical expressions for the reflectance can be obtained by the transfer matrix [see Eq. (49)],

$$\mathbf{M}^{(N)} = Q^{-1}\mathcal{M}^{(N)}Q. \tag{60}$$

After some algebra one can express the elements of the transfer matrix in terms of the parame ters of our model,

$$(\mathbf{M}^{(N)})_{1,1} = \frac{1}{\sin k \sin\mu}[\cos(2\mu N)\sin\mu\sin k - i\sin(2\mu N)(\cos\mu\cos k - \sin\beta)], \tag{61}$$

$$(\mathbf{M}^{(N)})_{1,2} = \frac{1}{\sin k \sin\mu}\{ie^{ik}\sin(2\mu N)[\sin(\beta + k) - \cos\mu]\}, \tag{62}$$

$$(\mathbf{M}^{(N)})_{2,1} = \frac{1}{\sin k \sin\mu}\{ie^{-ik}\sin(2\mu N)[\cos\mu - \sin(\beta - k)]\}, \tag{63}$$

$$(\mathbf{M}^{(N)})_{2,2} = \frac{1}{\sin k \sin\mu}[\cos(2\mu N)\sin\mu\sin k - i\sin(2\mu N)(\sin\beta - \cos\mu\cos k)]. \tag{64}$$

According to the definition, the right and left reflectances, R_R and R_L, are defined as follows,

$$R_R = \left|\frac{(\mathbf{M}^{(N)})_{1,2}}{(\mathbf{M}^{(N)})_{2,2}}\right|^2, \quad R_L = \left|\frac{(\mathbf{M}^{(N)})_{2,1}}{(\mathbf{M}^{(N)})_{2,2}}\right|^2. \tag{65}$$

Therefore, the reflectance for the wave incident from the right side of the system, one gets

$$R_R = \frac{[\cos\mu - \sin(\beta + k)]^2}{(\sin\beta - \cos\mu\cos k)^2 + [\cot(2\mu N)\sin\mu\sin k]^2}, \tag{66}$$

and for the wave incident from the left side we have

$$R_L = \frac{[\cos\mu - \sin(\beta - k)]^2}{(\sin\beta - \cos\mu\cos k)^2 + [\cot(2\mu N)\sin\mu\sin k]^2}. \tag{67}$$

For $\mathcal{PT}$-symmetric systems, the generalized relation between the transmittance and reflectances reads [32]

$$\sqrt{R_R R_L} = |1 - T|, \tag{68}$$

which is fulfilled for our model. Here T is the left or right transmittance of the system given by the definition, $T = 1/|(\mathbf{M}^{(N)})_{2,2}|^2$; see Eq. (48). As a check we see that when $\gamma \to 0$, both reflectances $R_{R,L} \to 0$ which is the expected result.

Let us now discuss the properties of R_R and R_L when γ is less, equal or larger than $\gamma_{\rm cr}$ which is defined by the relation, $E^2 + \gamma_{\rm cr}^2 = 4$. The data in Figs. 11 and 12 show the behavior of both reflectances for the above three cases, as a function of N. For $\gamma < \gamma_{\rm cr}$ both reflectances are periodic functions of N with the same resonant points at $N = m\pi/2\mu$, with m as

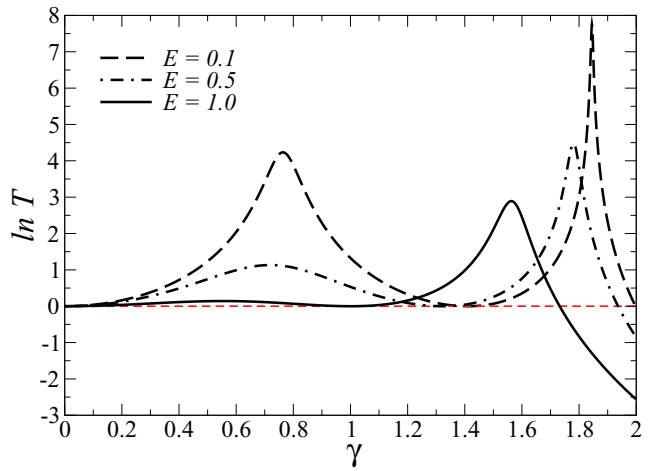

FIG. 10. (Color online) $\ln T$ versus γ for $N = 2$ and $E = 0.1, 0.5, 1.0$.

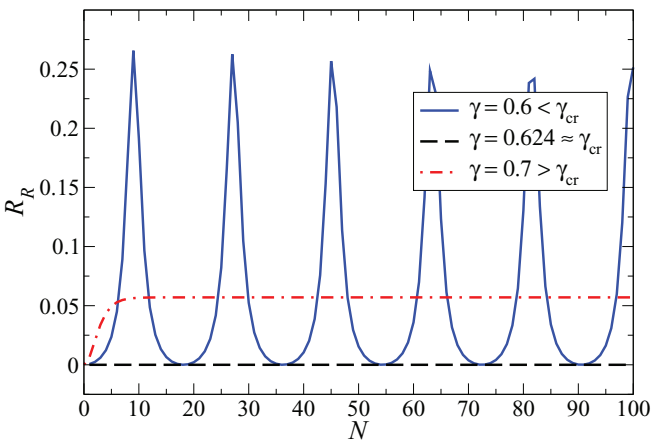

FIG. 11. (Color online) Right reflectance versus N for $E = 1.9$ and $\gamma = 0.6, 0.624, 0.7$, with $\gamma_{\rm cr} \approx 0.624$.

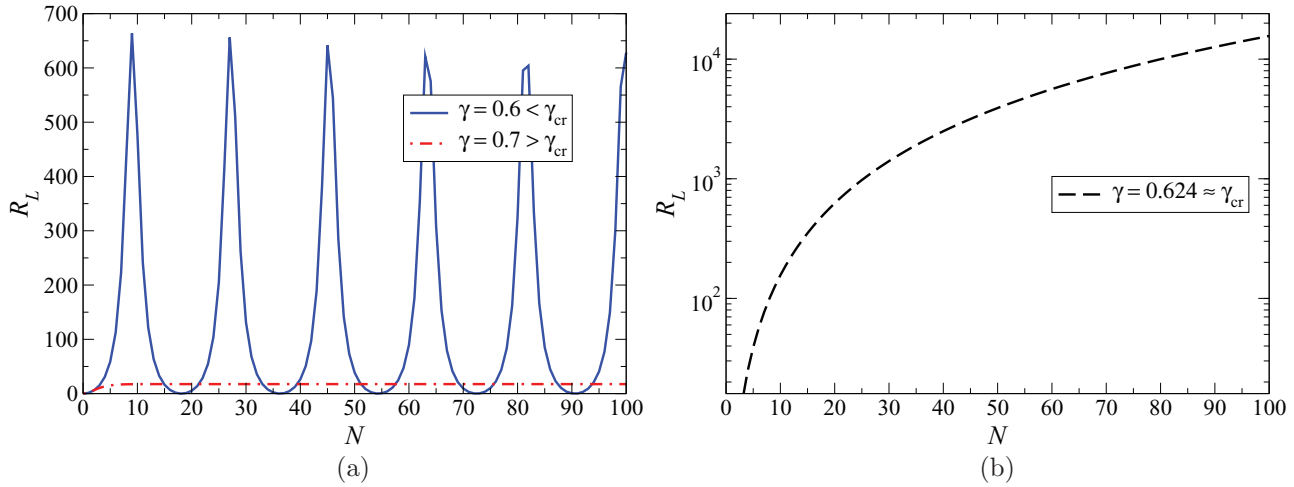

FIG. 12. (Color online) Left reflectance versus N for $E = 1.9$. (a) $\gamma = 0.6 < \gamma_{cr}$ and $\gamma = 0.7 > \gamma_{cr}$. (b) $\gamma = 0.624 \approx \gamma_{cr}$.

a positive integer. Of course, due to the relation (68) these points are equal to those when $T = 1$. For $\gamma = \gamma_{cr}$ one can see a very different behavior of both reflectances: While $R_R \approx 0$, the left reflectance R_L grows with N. In order to analyze this behavior one can use Eqs. (66) and (67). Note that these equations are not valid for the case when γ is exactly equal to γ_{cr}, nevertheless they give the correct limit. Specifically, taking $\mu \to 0$ we get $R_R \approx 0$ and $R_L \propto N^2$. This effect was termed *unidirectional reflectivity* in Ref. [24] where the authors have studied the $\mathcal{PT}$-symmetric model with finite width of barriers. When $\gamma > \gamma_{cr}$ one can observe that both reflectances approach a constant value quite rapidly, the fact that can be easily deduced from Eqs.(66) and (67).

Figure 13 shows the dependence of the reflectances with respect to E. From these data as well as from Eqs. (66) and (67), one can see that when $|E| \to 2$, both reflectances, $R_{R,L} \to 1$. Due to the fact that the dependence on E is different for both reflectances they show a different number of points where they vanish. Indeed, while for R_R the vanishing points are the same that the ones corresponding to the resonant values of T [see Eq. (58)] for R_L this holds only when $E^2 + \gamma^2 < 4$. The resonant value of T for $E^2 + \gamma^2 = 4$ corresponds to an increase in R_L, not to a local maximum, and to vanishing of R_R. This is due to the fact that at this point we have $\cos\mu - \sin(\beta + k) = 0$ and $\cos\mu - \sin(\beta - k) = 2\sin^2 k$.

D. Discussion

The approach which we have used in this paper allows us to relate the properties of spectra and eigenstates for the "bounded" model to the structure of scattering states for the "unbounded" model, as well as to the properties of transmission and reflection for finite samples attached to perfect leads. The key ingredient for the relation between the two models is the expression (10) determining the energy spectrum in the bounded model. This expression has to be compared with Eq. (41) which defines the parameter μ emerging in the unbounded model. One can see that both expressions have the same structure, however, they have different meaning. In the first case (the bounded model) the

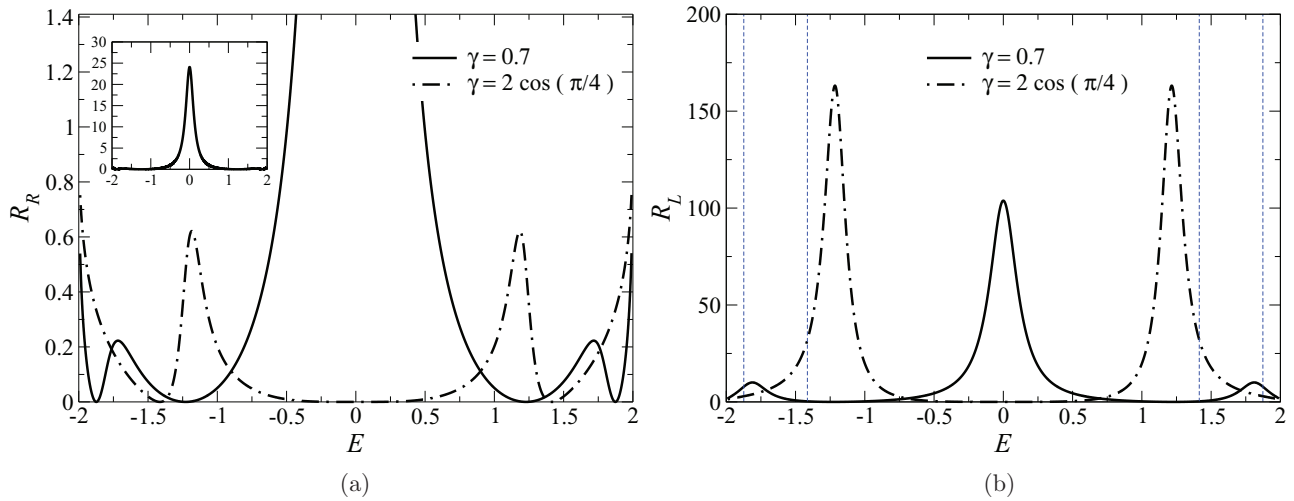

FIG. 13. (Color online) (a) Right reflectance versus E for $\gamma = 0.7$ and $\gamma = 2\cos(\pi/4)$ where the latter corresponds to the resonant value of T at the band center, $N = 2$. Inset shows full plot for $\gamma = 2\cos(\pi/4)$. (b) Left reflectance versus E for the same parameters as in (a). Here vertical lines mark the points where $E^2 + \gamma^2 = 4$.

energies E_s are determined by the parameter γ and by the wave vector k_s emerging due to the zero or periodic boundary conditions. To the contrary, in the unbounded model the energy E is a free parameter corresponding to the energy of an incident wave in the scattering problem, and the parameter μ emerges in place of k_s. In infinite periodic systems without gain this parameter μ can be associated with the well-known Bloch index. In such systems the Bloch index defines the band structure for energies of propagating waves, as well as the properties of evanescent waves that decrease exponentially fast along the structure.

One of our interests is how the Bloch-like index μ enters the expression for the scattering states for any finite N. We show that when μ is real, the scattering states are extended inside the sample of size N, and μ can be treated as the wave vector. A completely different situation occurs for the imaginary values of μ, for which the scattering states consist of two components; one is an exponentially increasing function of the site index n and another is an exponentially decreasing function of n. This fact is extremely important in view of the value of the transmission coefficient T. It turns out that the specific boundary conditions corresponding to the scattering problem [see Eq. (35)] result in the asymmetry for exponentially increasing or decreasing components in the scattering states. This fact directly leads to the exponential decrease of T in the limit of large N. As a result, one can formally introduce the localization length ℓ_∞ in the same way as it is done in the theory of disordered models [see Eq. (47)]. In Sec. IV we have shown that the same value of localization length can be obtained by analyzing the structure of scattering states.

It should be noted that an emergence of the exponential decrease of the transmission coefficient T in the limit of large N is known to occur in one-dimensional models with either gain or loss only [32,37–46]. In both cases two eigenvalues $\lambda_{1,2}$ of the transfer matrix $\mathcal{M}$ corresponding to the periodic cell, are related to each other due to the simple relation, $\lambda_1\lambda_2 = 1$. In the absence of gain or loss, the two eigenvalues are complex with modulo one which corresponds to real values of μ. On the other hand, in the presence of either gain or loss the two eigenvalues are real with $\lambda_1 = 1/\lambda_2$. This means that the scattering states consist of two terms; one is exponentially growing with n and the other decreases exponentially with n. The surprising fact is that the boundary conditions *at one side* of a sample (specifically, at two sites) effectively select one component which prevails in the limit $N \to \infty$ [see Eq. (46)], and, therefore, result in an exponential *decrease* of the transmission coefficient, for *both* cases, either for gain or loss.

From our analysis it is clear that the value of the localization length, if it is defined for large enough N in the formal way (either from the structure of scattering states or due to the logarithm $\ln T$ of the transmission coefficient), can be obtained simply from the expression for the Bloch-like index μ. As we have shown, it can be done due to the relation,

$$\frac{1}{\ell_\infty} = 2|\mu|, \quad \cosh^2|\mu| = \frac{1}{4}(E^2+\gamma^2), \tag{69}$$

for μ imaginary. The generalization of this relation is straightforward for any kind of model allowing to be expressed by the transfer matrix describing *one* periodic cell. In our case, the basic cell consists of two sites, however, in general it could consist of any number of sites. Then, having the expression for μ one can easily obtain the localization length ℓ_∞ from the first relation in Eq. (69). The same approach can be used for more complicated periodic cells in the model, for example, with different amount γ_1 of gain and γ_2 of loss. Note that the presence of the $\mathcal{PT}$ symmetry is not important for such an analysis. As is now clear, the $\mathcal{PT}$ symmetry allows one to have a quite specific situation with real eigenvalues of energy for the eigenstates which is equivalent to real values of the Bloch-like parameter μ for scattering states.

One has to emphasize that although the index μ can be formally treated as the common Bloch index that emerges in periodic structures with real potentials (with or without disorder), its role is quite specific in the models with gain. Indeed, as was found for the Anderson model with the gain at each site and without the loss [42–46], the exponential *decrease* of the transmission coefficient occurs in the strong limit $N \gg N_{\rm cr}$ where $N_{\rm cr}$ depends on the energy and the gain parameter γ; for small γ this critical size $N_{\rm cr}$ is very large. As for $N < N_{\rm cr}$, the transmission coefficient T exponentially *increases*. This relatively simple model demonstrates that there is a strong competition between the increasing and decreasing components in the structure of scattering states. For this reason the role of the index μ is basically different from that of the Bloch index characterizing the models without the gain. As is well known, in such models the Bloch index is associated with evanescent modes. The latter emerge in 1D disordered models for which all scattering properties are defined by the backscattering length only. This is not the case for the models with gain, and the exponentially increasing component of the scattering states should not be neglected. As one can see, the knowledge of the "localization length" ℓ_∞ discussed above is far from being enough to predict the dependence of T on N. Thus, the problem of finding an expression for the transmission coefficient T is of a high importance. Our analytical results clearly demonstrate a quite complicated dependence of the transmission coefficient on the control parameter γ, energy E and the length N of the scattering structure. More details can be seen in Fig. 8 demonstrating that for $N < N_{\rm cr} \sim 1/|\mu|$ the transmission coefficient is basically described by two components, increasing and decreasing ones.

One of the central results of our study is a quite simple expression for the transmission coefficient T; see Eq. (52). It is rigorously obtained for *any* value of γ and N and any value of energy E of an incident wave. This expression allows one to analyze various situations emerging in the scattering. It shows that for real value of μ for which $\gamma < \gamma_{\rm cr}$ the transmission coefficient T is larger than 1, apart from specific values of N for which $T = 1$. On the contrary, for imaginary μ corresponding to $\gamma > \gamma_{\rm cr}$, the value of T is less than 1. This is related to the onset of localization of scattering states as is shown in Sec. IV A. At the exceptional point $\mu = 0$ with $\gamma = \gamma_{\rm cr}$, the transmission is perfect, $T = 1$, and, together with the vanishing change of phase for the scattering states, this leads to the invisibility of the structure [47]. Although this effect emerges only for specific values of energy E, from Fig. 9 one can see that the transmission coefficient is very close to unity in a quite large region of E.

As for the reflectance, our results show an emergence of "unidirectional reflectivity" observed in Ref. [24] for the $\mathcal{PT}$-symmetric model with a finite width of barriers. This effect is more pronounced for large values of N. The analytical expressions give full information about the difference between left and right reflectances in dependence on the model parameters.

In conclusion, our analytical results reveal the mechanism for the emergence of the localized scattering states which is entirely due to the presence of the gain or loss terms in the non-Hermitian Hamiltonian. It should be stressed that the onset of such a localization is not related to the $\mathcal{PT}$ symmetry; it emerges due to the imaginary value of the Bloch-like parameter μ. This conclusion is quite general and can occur in any non-Hermitian model, thus allowing one to express the localization in terms of this parameter μ only. The role of the $\mathcal{PT}$ symmetry is just to have three regimes in the same model, governed by the value of μ (or, the same, by the relation between E and γ). These three regimes are as follows: the transmission with $T > 1$ due to extended scattering states, perfect transmission for $\mu = 0$ and any N (resulting in the invisibility), and the regime with $T < 1$ emerging due to localized scattering states.

ACKNOWLEDGMENTS

F.M.I. is thankful to L. I. Deych, A. A. Lisyansky, N. M. Makarov, V. V. Sokolov, and V. G. Zelevinsky for fruitful discussions; he also acknowledges the support from CONACyT Grants No. N-161665 and No. 133375. The work of D.N.C. was partially supported by NSF Grant No. ECCS-1128520 and AFOSR Grant No. FA95501210148.

[1] N. W. Ashcroft and N. D. Mermin, in *Solid State Physics*, edited by F. Seitz and D. Turnbull (Brooks-Cole, Belmont, 1976).
[2] O. Morsch and M. Oberthaler, Rev. Mod. Phys. **78**, 179 (2006).
[3] E. Yablonovitch, T. J. Gmitter, R. D. Meade, A. M. Rappe, K. D. Brommer, and J. D. Joannopoulos, Phys. Rev. Lett. **67**, 3380 (1991).
[4] D. N. Christodoulides, F. Lederer, and Y. Silberberg, Nature (London) **424**, 817 (2003).
[5] C. M. Bender and S. Boettcher, Phys. Rev. Lett. **80**, 5243 (1998); C. M. Bender, D. C. Brody, and H. F. Jones, *ibid.* **89**, 270401 (2002); C. M. Bender, Rep. Prog. Phys. **70**, 947 (2007).
[6] G. Levai and M. Znojil, J. Phys. A **33**, 7165 (2000); A. Mostafazadeh, J. Math. Phys. (N.Y.) **43**, 205 (2002); Z. Ahmed, Phys. Lett. A **282**, 343 (2001).
[7] R. El-Ganainy, K. G. Makris, D. N. Christodoulides, and Z. H. Musslimani, Opt. Lett. **32**, 2632 (2007).
[8] K. G. Makris, R. El-Ganainy, D. N. Christodoulides, and Z. H. Musslimani, Phys. Rev. Lett. **100**, 103904 (2008).
[9] Z. H. Musslimani, K. G. Makris, R. El-Ganainy, and D. N. Christodoulides, Phys. Rev. Lett. **100**, 030402 (2008).
[10] S. Klaiman, U. Günther, and N. Moiseyev, Phys. Rev. Lett. **101**, 080402 (2008).
[11] A. Guo, G. J. Salamo, D. Duchesne, R. Morandotti, M. Volatier-Ravat, V. Aimez, G. A. Siviloglou, and D. N. Christodoulides, Phys. Rev. Lett. **103**, 093902 (2009).
[12] C. E. Rüter, K. G. Makris, R. El-Ganainy, D. N. Christodoulides, M. Segev, and D. Kip, Nature Phys. **6**, 192 (2010).
[13] A. Regensburger, C. Bersch, M. A. Miri, G. Onishchukov, D. N. Christodoulides, and U. Peschel, Nature (London) **488**, 167 (2012).
[14] A. Regensburger, M. A. Miri, C. Bersch, J. Nager, G. Onishchukov, D. N. Christodoulides, and U. Peschel, Phys. Rev. Lett. **110**, 223902 (2013).
[15] M. A. Miri, A. Regensburger, U. Peschel, and D. N. Christodoulides, Phys. Rev. A **86**, 023807 (2012).
[16] L. Feng, Y. L. Xu, W. S. Fegadolli, M. H. Lu, J. B. E. Oliveira, V. Almeida, Y. F. Chen, and A. Scherer, Nat. Mater. **12**, 108 (2013).
[17] S. Longhi, Phys. Rev. Lett. **103**, 123601 (2009); Phys. Rev. A **82**, 031801(R) (2010).
[18] M. C. Zheng, D. N. Christodoulides, R. Fleischmann, and T. Kottos, Phys. Rev. A **82**, 010103(R) (2010).
[19] H. Ramezani, T. Kottos, R. El-Ganainy, and D. N. Christodoulides, Phys. Rev. A **82**, 043803 (2010).
[20] H. Schomerus, Phys. Rev. Lett. **104**, 233601 (2010); Phys. Rev. A **83**, 030101(R) (2011).
[21] A. A. Sukhorukov, Z. Xu, and Y. S. Kivshar, Phys. Rev. A **82**, 043818 (2010).
[22] A. E. Miroshnichenko, B. A. Malomed, and Y. S. Kivshar, Phys. Rev. A **84**, 012123 (2011).
[23] Y. D. Chong, Li Ge, and A. Douglas Stone, Phys. Rev. Lett. **106**, 093902 (2011).
[24] Z. Lin, H. Ramezani, T. Eichelkraut, T. Kottos, H. Cao, and D. N. Christodoulides, Phys. Rev. Lett. **106**, 213901 (2011).
[25] M.-A. Miri, P. LiKamWa, and D. N. Christodoulides, Opt. Lett. **37**, 764 (2012).
[26] M. Liertzer, Li. Ge, A. Cerjan, A. D. Stone, H. E. Türeci, and S. Rotter, Phys. Rev. Lett. **108**, 173901 (2012).
[27] Y. N. Joglekar and J. L. Barnett, Phys. Rev. A **84**, 024103 (2011); H. Vemuri, V. Vavilala, T. Bhamidipati, and Y. N. Joglekar, *ibid.* **84**, 043826 (2011).
[28] E. M. Graefe and H. F. Jones, Phys. Rev. A **84**, 013818 (2011).
[29] D. A. Zezyulin and V. V. Konotop, Phys. Rev. Lett. **108**, 213906 (2012).
[30] H. Schomerus, Phil. Trans. R. Soc. A **371**, 20120194 (2013).
[31] P. Ambichi, K. G. Makris, Li Ge, Y. Chong, A. D. Stone, and S. Rotter, Phys. Rev. X **3**, 041030 (2013).
[32] Li Ge, Y. D. Chong, and A. D. Stone, Phys. Rev. A **85**, 023802 (2012).
[33] P. Markos and C. M. Soukoulis, *Wave Propagation. From Electrons to Photonic Crystals and Left-Handed Materials* (Princeton University Press, Princeton, 2008).
[34] O. Bendix, R. Fleischmann, T. Kottos, and B. Shapiro, Phys. Rev. Lett. **103**, 030402 (2009).
[35] H. Ramezani, D. N. Christodoulides, V. Kovanis, I. Vitebskiy, and T. Kottos, Phys. Rev. Lett. **109**, 033902 (2012).
[36] S. Weigert, Phys. Rev. A **68**, 062111 (2003).
[37] A. K. Gupta and A. M. Jayannavar, Phys. Rev. B **52**, 4156 (1995).

[38] J. C. J. Paasschens, T. Sh. Misirpashaev, and C. W. J. Beenakker, Phys. Rev. B **54**, 11887 (1996).
[39] T. Sh. Misirpashaev, J. C. J. Paasschens, and C. W. J. Beenakker, Physica A **236**, 189 (1997).
[40] S. K. Joshi and A. M. Jajannavar, Phys. Rev. B **56**, 12038 (1997).
[41] N. Natano and D. Nelson, Phys. Rev. B **58**, 8384 (1998).
[42] X. Jiang and C. M. Soukolis, Phys. Rev. B **59**, 6159 (1999).
[43] X. Jiang, Q. Li, and C. M. Soukoulis, Phys. Rev. B **59**, R9007 (1999).
[44] Sandeep K. Joshi and A. M. Jayannavar, Int. J. Mod. Phys. B **14**, 1669 (2000).
[45] J. Heinrichs, J. Phys.: Condens. Matter **18**, 4781 (2006).
[46] P. K. Datta, Phys. Rev. B **59**, 10980 (1999).
[47] A. Mostafazadeh, Phys. Rev. A **87**, 012103 (2013).